Tactile sensor array using microcantilever with nickel-chromium alloy thin film of low temperature coefficient of resistance and its application to slippage detection

Masayuki Sohgawa[a,1], Daiki Hirashima[a], Yusuke Moriguchi[a], Tatsuya Uematsu[a], Wataru Mito[b], Takeshi Kanashima[a], Masanori Okuyama[a], Haruo Noma[b]

[a]*Osaka University, 1-3 Machikaneyama-cho, Toyonaka, Osaka 560-8531, JAPAN*
[b]*Advanced Telecommunications Research Institute International, 2-2-2 Hikari-dai, Seika, Souraku, Kyoto 619-0288, JAPAN*

Abstract

A tactile sensor consisting of microcantilevers has been fabricated using the NiCr-thin-film strain gauge with low noise by surface micromachining and the slippage has been detected by using the fabricated tactile sensor array. The NiCr alloy thin film of Cr: 75wt% has very low temperature coefficient of resistance (TCR) and is employed to suppress the temperature noise and drift. The fabricated tactile sensor with the NiCr thin film (Cr: 75wt%) has linear dependencies of the resistance on normal and shear forces, and shows lower noise and temperature drift than that with conventional NiCr (Cr: 20wt%) film. Normal and shear forces measured by fabricated sensor well coincide with applied forces with errors of 3–3.5 kPa. Moreover, the gripping status of the robotic hand was detected by using fabricated tactile

Email address: `sohgawa@ee.es.osaka-u.ac.jp` (Masayuki Sohgawa)
[1]Tel: +81-6-6850-6331, Fax: +81-6-6850-6341

sensor array, and the slipping condition can be judged at the rate of 76.5%.
Keywords:
tactile sensor, nickel chromium, slippage detection, microcantilever, elastomer, temperature coefficient of resistance

---

1. Introduction

Recently, human-support robots for the nursing care in an aging society gather much attentions [1]. Additionally, industrial robots with dexterous manipulation skills have been expected for use in assembly factories instead of humans [2, 3]. To achieve the dexterous action of these robots, precise detection of objects is required, however, current conventional sensors such as optical, sonic, and pressure sensors remain insufficient [4, 5]. Thus, high-density tactile sensors with detection ability for normal and shear forces and with soft surfaces like the human hand are required. Human beings can detect normal and shear forces by tactile organs on finger tips [5]. Moreover, the tactile sense of human beings has wide range of the sensitivity from tens Pa to hundreds kPa and spacial resolution of 2 mm at finger tips. Many kinds of tactile sensors have already been proposed [4, 5, 6, 7, 8, 9, 10, 11, 12]. However, high-density tactile sensor arrays that can simultaneously detect normal and shear forces using one sensor element have not been realized yet.

We have proposed a tactile sensor with micro-cantilevers embedded in the elastomer (polydimethylsiloxane; PDMS) for these robots and fabricated by microelectromechanical systems (MEMS) technologies. It is demonstrated that the fabricated tactile sensors can detect normal and shear forces simultaneously, in the previous works [13, 14, 15, 16, 17]. Although temperature drift or noise is a serious problem, these can be reduced by using a NiCr thin film as reported in [18]. However, it is expected that the Ni:Cr ratio in the NiCr thin film and fabrication of the microcantilever structure influence the temperature property of fabricated sensors.

In this work, we have investigated a temperature dependence of the resistance of sputtered NiCr thin films and fabricated the tactile sensor array using the NiCr film with weak temperature dependence. Moreover, a fabricated tactile sensor array has been applied to slippage detection in holding the object by robot hands.

2. The structure and detection principle of the tactile sensor element

Figure 1 (a) shows an element structure of the proposed tactile sensor. One tactile sensor element is composed of three microcantilevers embedded in an elastomer. The cantilever has an inclined shape caused by residual stress in thin films formed on it so that it can deform both perpendicularly and horizontally to the sensor surface. The thin-film strain gauge is set up on the cantilever.

Figure 1 (b) shows a cross-sectional structure of the microcantilever with length of 300 μm. The microcantilever was fabricated by the surface micromachining process using a silicon-on-insulator (SOI) wafer and has an inclined shape because of residual tensile stress in the Cr or Cytop (Asahi Glass Co., Ltd.) layer. A tactile sensor element is composed of three cantilevers and is embedded in the PDMS. Applied force is detected as the resistance change of NiCr-thin-film strain gauge deposited by rf-sputtering and patterned on the microcantilever. When normal force is applied at the surface of the PDMS, the microcantilever is deformed downward, so the resistance of the strain gauge changes. On the other hand, when shear force is applied from right to left in Fig. 1 (b), the microcantilever is deformed upward, so the resistance decreases. In contrast, the microcantilever is deformed downward by shear force applied from left to right in Fig. 1 (b). Thus, the amplitude and direction of applied force can be obtained from the resistance change. Ratio of the resistance change, $\Delta R/R$, is expressed by the summation of a linear combination of normal and shear forces as

$$\Delta R/R = k_x F_x + k_y F_y + k_z F_z, \tag{1}$$

where k_x, k_y, and k_z are the sensitivities of the cantilever to F_x, F_y, and F_z, respectively [19]. The ratio obtained from three differently directed cantilevers, which have different sensitivities to force in each axis, are shown as

$$\begin{pmatrix} \Delta R_1/R_1 \\ \Delta R_2/R_2 \\ \Delta R_3/R_3 \end{pmatrix} = \begin{pmatrix} k_{1x} & k_{1y} & k_{1z} \\ k_{2x} & k_{2y} & k_{2z} \\ k_{3x} & k_{3y} & k_{3z} \end{pmatrix} \begin{pmatrix} F_x \\ F_y \\ F_z \end{pmatrix}. \tag{2}$$

Thus, once the sensitivities k_x, k_y, and k_z are obtained in advance, the normal and shear forces can be calculated by solving simultaneous equations with three unknown resistance changes:

$$\begin{pmatrix} F_x \\ F_y \\ F_z \end{pmatrix} = \begin{pmatrix} k_{1x} & k_{1y} & k_{1z} \\ k_{2x} & k_{2y} & k_{2z} \\ k_{3x} & k_{3y} & k_{3z} \end{pmatrix}^{-1} \begin{pmatrix} \Delta R_1/R_1 \\ \Delta R_2/R_2 \\ \Delta R_3/R_3 \end{pmatrix}. \tag{3}$$

3. Fabrication Process

A silicon-on-insulator (SOI) wafer was used as a substrate. The thicknesses of the Si substrate, buried oxide, and thin Si layers are 500, 1, and 2.5 μm, respectively. Firstly, a Si_3N_4 thin film (thickness: 300 nm) was deposited as an insulating layer by the low-pressure chemical vapor deposition (LPCVD) method. Then, a NiCr alloy thin film (thickness: 50 nm) was deposited by the sputtering method. Percentage of the Cr in the target is 10–100wt%. A Au/Cr layer (thickness: 200/40 nm) was also formed as the electrode by the sputtering method. A Cr or a Cytop thin film was used to bend the cantilever structure upward. The Cr film (thickness: 200 nm) was deposited by electron beam (EB) evaporation. On the other hand, the Cytop film (thickness: 6 μm) was spin-coated and cured at 200°C for 1 hour. Finally, the cantilever structure was formed by the sacrificial etching of the buried oxide layer in buffered hydrofluoric acid (BHF) solution (NH_4HF_2: 20%) for 5 hours, and then dried in vacuum after rinsing in ultrapure water and then in ethanol. The Si_3N_4, NiCr, Au, Cr, and Cytop films have enough durability against BHF solution for 5 hours. The etching time is controlled by using etching marker which is peeled off when the microcantilever is released from the substrate.

The microcantilevers were covered with PDMS (Silpot184; Toray Dow Corning) using a plastic mold form. Curing temperature and time of PDMS are 120°C and 2 hours, respectively. The height of the PDMS were 1 mm. An optical and electronic microscopic images of the fabricated tactile sensor is shown in Fig. 2. The tip height of the microcantilevers are 30–40 μm. The size of the sensor chip is 3×4 mm.

4. Temperature dependence of resistance in NiCr thin film

The resistance of the NiCr thin film was measured by a digital multimeter in the thermostatic oven at 40–80°C. The resistance change is almost propotional to the temperature. Temperature coefficient of resistance (TCR) can be obtained as gradient of the fitted line. Figure 3 shows TCR of the NiCr thin film (thickness: 50 nm) deposited by rf-magnetron sputtering as a function of Cr weight concentration of the sputtering target before (cross) and after (open circle) releasing the cantilever from the substrate. The error bar in Fig. 3 shows standard deviation of data. It is found that TCR heavily depends on the Ni:Cr ratio. TCR of NiCr thin film has small value from Cr: 40wt% to 75wt% and has the least value around Cr: 75wt%. Moreover, TCR of the NiCr thin film increases at 30 ppm/K on average after releasing of the cantilever independently of Cr concentration. It is considered that TCR of the NiCr film increases after release of the cantilever because the resistance increases with increasing tensile strain induced by the bimetallic effect.

Considering the bimetallic structure model as shown Fig. 4, the change of curvature radius, ρ, of the microcantilever induced by bimetallic effect at temperature change ΔT can be calculated by a following equation [20],

$$\rho = \frac{hK}{6\left(\alpha_1 - \alpha_2\right)\Delta T}, \tag{4}$$

where α_1 and α_2 are coefficients of thermal expansion of the top and bottom layers, respectively, h is the total thickness and K is a parameter:

$$K = 3 + s_1^2 + s_2^2 + \frac{\omega s_2^2}{s_1} + \frac{s_1^3}{\omega s_2}, \tag{5}$$

$$s_1 = \frac{h_1}{h}, s_2 = \frac{h_2}{h}, \omega = \frac{E_2}{E_1}, \tag{6}$$

where h_1 and h_2 are thicknesses of the top and bottom layers, and E_1 and E_2 are Young's moduli of the top and bottom layers, respectively. Increase of tensile strain, $\Delta\varepsilon$, is expressed as a following equation [21],

$$\Delta\varepsilon = \frac{t}{\rho} = \frac{6(\alpha_1 - \alpha_2)t}{hK}\Delta T, \tag{7}$$

where t is distance from neutral plane of the microcantilever. Therefore, using the gauge factor k of the strain gauge (~ 2), the resistance change by the bimetallic effect can be calculated as follows,

$$\frac{\Delta R}{R} = k\Delta\varepsilon = \frac{6k(\alpha_1 - \alpha_2)t}{hK}\Delta T. \tag{8}$$

Although an actual structure of the cantilever is shown in Fig. 1 (b), the Si_3N_4 and the NiCr layers can be negligible because its thickness is much thinner than other layers. Table 1 shows the material parameters of Cytop and Si to calculate eq. 8. The apparent increase of the resistance per unit temperature is calculated as 31 ppm/K using the values in Table 1. This value is almost same to measured one, so it is clear that increase of resistance after releasing the microcantilever is caused by the bimetallic effect.

Figure 5 shows TCR of the NiCr thin film (Cr: 75wt%) before and after releasing the cantilever from the substrate, and that after embedded in the PDMS. After embedding the microcantilever in PDMS, TCR decreases to pretty low level again; however increase of TCR is remain (residual increase) because of thermal expansion of the PDMS. Therefore, it is considered that the elastomer material which has low coefficient of thermal expansion plays a adequate role to improve temperature characteristics furthermore.

5. Results and discussion

5.1. Force measurements by fabricated tactile sensors

Normal force was applied to the surface of the fabricated tactile sensor by the metal rod attached to z-axis stage. Shear force was applied by moving of x- and y-axis stages. Applied forces were measured by a conventional 6-axis force sensor (Nitta; UFS 2A-05). The resistance change was measured by a precision digital multimeter (Advantest; R6581). Figures 6 (a) and (b) show rates of the resistance change of the tactile sensors using the NiCr thin films (Cr: 20wt% and 75wt%) as a function of applied normal and shear forces, respectively. Force was increased from 0 to the maximum value, and then decreased from the maximum value to 0. The measurement was repeated 3 times. Initial resistances of the Cr: 20wt% and Cr: 75wt% films without applying force is about 1.4 kΩ and 2.5 kΩ, respectively. Linear dependencies of the resistance on both normal and shear forces are obtained. However, the tactile sensor using the NiCr (Cr: 20wt%) film has large temperature noise and drift than that of Cr: 75wt% film. TCR of the NiCr (Cr: 75wt%) film (4 ppm/K) is lower than that of the NiCr (Cr: 20wt%) film (140 ppm/K), so it is showed that the signal noise caused by temperature fluctuation can be drastically reduced by using NiCr (Cr: 75wt%) film instead of the NiCr (Cr: 20wt%) film.

Figures 7 (a) and (b) show comparisons between applied and measured normal and shear forces in fabricated tactile sensor with the NiCr thin film of Cr: 20wt% (in the previous work [19]) and 75wt%, respectively. For the tactile sensor using the NiCr (Cr: 20wt%), the average values of error between applied and measured forces are 5.9 kPa for F_x, 4.7 kPa for F_y, and 32 kPa for F_z, respectively. On the other hand, for the tactile sensor using the NiCr of Cr: 75wt%, the average values of error between applied and measured forces are 3.0 kPa for F_x, 3.1 kPa for F_y, and 3.5 kPa for F_z, respectively. Thus, the error of measured force vector can be also reduced by using NiCr (Cr: 75wt%) film instead of the NiCr (Cr: 20wt%) film, and it is confirmed that normal and shear forces can be simultaneously detected with errors of 3–3.5 kPa.

5.2. Slippage detection using fabricated tactile sensors

Detection of slippage condition in the case of gripping of an acrylic object by the robotic hand was performed by using the fabricated tactile sensor array. Figure 8 shows a test system for slippage detection. The fabricated tactile sensor array is attached to the robotic hand ((a) in Fig. 8). A camera is set in the acrylic object ((b) in Fig. 8) to monitor the gripping state through a mirror ((c) in Fig. 8). The reference force is monitored by a conventional force sensor ((d) in Fig. 8). The robotic hand grips and holds up an acrylic object, and then grip of the hand is loosened so that the object slips by gravity force. The weight of the acrylic object was about 300 g. The sensor output was precisely measured by using the Wheatstone bridge circuit as shown in Fig. 9. Reference resistances were also formed on wafer. As the resistance change is extremely small, the output voltage V_o is expressed by a following equation [22],

$$V_o = \frac{1}{4}\frac{\Delta R}{R_0}V_i, \tag{9}$$

where V_i, ΔR, and R_0 is source voltage supplied to the Wheatstone bridge circuit, the change of resistance by external force application, and resistance without force, respectively. The output voltage from the Wheatstone bridge was amplified by LSI amplifiers (ATC-LSI; AT-1051). The detection rate of the output is 100 Hz. Number of the sampling data is 11,000 and the measurement time is 110 sec.

The amplified output voltage of the fabricated tactile sensor changes depending on the gripping state as shown in Fig. 10. The gripping state were monitored by a camera set in the acrylic object. The sensor output changes depending on change of the gripping state. In particular, an attention should be paid to the fact that the sensor output oscillates in the slipping state. It is considered that this oscillation of the sensor output is caused by the stick-slip phenomena.

The gripping status was classified by the outputs of two sensor elements by using the k-Nearest Neighbor method [23, 24]. The detection rate of the gripping status was 98.8% for the non-contact state, 33.3% for the gripping state (with pressing), 96.0% for the griping state (in stable), and 76.5% for the slipping state, respectively. The no-contact and stable gripping states can be discriminated almost perfectly. Moreover, the slipping state can be detected with a relatively high accuracy. On the other hand, the precision rate for detection of the gripping state with pressing is quite lower than that of other states. It is considered that the surface of the tactile sensor on the robotic hand partially contacts with the object so that it needs the information from more points of the tactile sensor to detect this state. Nevertheless, it is demonstrated that the fabricated tactile sensor array can be used the slippage detection.

6. Conclusion

We have fabricated a tactile sensor using the microcantilever with the NiCr thin film embedded in the PDMS. The NiCr (Cr: 75wt%) thin film has quite low temperature coefficient of resistance so that temperature noise and drift can be decreased by using it. The output of the tactile sensor using the NiCr (Cr: 75wt%) film has good linearity and low noise so that resolution of forces are improved to 3.0 kPa for F_x, 3.1 kPa for F_y, and 3.5 kPa for F_z, respectively. Moreover, detection of slippage between the robotic hand and an acrylic object was performed by using fabricated tactile sensor array, and slipping condition can be detected at the rate of 76.5%.

References

[1] M. Onishi, Z. L̃uo, T. Odashima, S. Hirano, K. Tahara, T. Mukai, Generation of Human Care Behaviors by Human-Interactive Robot RI-MAN, 2007 IEEE Int. Conf. on Robotics and Automation, Roma, Italy, April 10–14 (2007) 3128–3129.

[2] M. Fujii, W. Inamura, H. Murakami, K. Tanaka, K. Kosuge, Cooperative Control of Multiple Mobile Robots Transporting a Single Object with Loose Handling, Proc. 2007 IEEE. Int. Conf. Robotics Biomimetics (2007) 816–822.

[3] K. Noda, Y. Hashimoto, Y. Tanaka, I. Shimoyama, MEMS on Robot Applications, Transducers 2009, Denver CO, USA (2009) 2176–2181.

[4] M. H. Lee, H. R. Nicholls, Tactile sensing for mechatronics – a state of the art surveyMechatronics 9 (1999) 1–31.

[5] R. S. Dahiya, G. Metta, M. Valle, G. Sandini, Tactile sensing-from humans to humanoids, IEEE Trans. Robotics 26 (2010) 1–20.

[6] Z. Chu, P. M. Sarro, S. Middelhoek, Silicon three-axial tactile sensor, Sens. Actuators A 54 (1996) 505–510.

[7] K. Noda, K. Hoshino, K. Matsumoto, and I. Shimoyama, A shear stress sensor for tactile sensing with the piezoresistive cantilever standing in elastic material, Sens. Actuators A 127 (2006) 295–301.

[8] D. J. Heever, K. Schreve, C. Scheffer, Tactile Sensing Using Force Sensing Resistors and a Super-Resolution Algorithm, IEEE Sens. J. 9 (2009) 29–35.

[9] C.-S. Park, J. Park, D. -W. Lee, A piezoresistive tactile sensor based on carbon fibers and polymer substrates, Microeletron. Eng. 86 (2009) 1250–1253.

[10] Y.-C. Liu, C.-M. Sun, L.-Y. Lin, M.-H. Tsai, and W. Fang, A tunable range/sensitivity CMOS-MEMS capacitive tactile sensor with polymer fill-in technique, Transducers 2009, Denver CO, USA (2009) 2190–2193.

[11] M. Shimojo, T. Araki, A. Ming, M. Ishikawa, A High-Speed Mesh of Tactile Sensors Fitting Arbitrary Surfaces, IEEE Sens. J. 10 (2010) 822–830.

[12] C.-S. Kim, B. K. Kang, J. H. Jung, M. J. Lee, H. B. Kim, S. S. Oh, S. H. Jang, H. J. Lee, H. Kastuyoshi, J. K. Shin, Active Matrix Touch Sensor Perceiving Liquid Crystal Capacitance with Amorphous Silicon Thin Film Transistors, Jpn. J. Appl. Phys. 49 (2010) 03CC03.

[13] M. Sohgawa, Y. M. Huang, T. Kanashima, K. Yamashita, M. Noda, M. Okuyama, H. Noma, Fabrication and Characterization of Silicon-Polymer Beam Structures for Cantilever-Type Tactile Sensors, Transducers '07, Lyon, France (2007) 1461–1464.

[14] M. Sohgawa, Y. -M. Huang, M. Noda, T. Kanashima, K. Yamashita, M. Okuyama, M. Ikeda, H. Noma, Fabrication and Characterization of Normal and Shear Stresses Sensitive Tactile Sensors by using Inclined Micro-cantilevers Covered with Elastomer, Mater. Res. Soc. Symp. Proc. 1052 (2008) 151–156.

[15] M. Sohgawa, H. Onishi, T. Mima, Y. -M. Huang, T. Kanashima, K. Yamashita, M. Noda, M. Okuyama, M. Ikeda, H. Noma, Detection of Normal and Shear Stresses by Tactile Sensors with Piezoresistive Micro-cantilever and Elastomer, Asia-Pacific Conf. on Transducers and Micro-Nano Tech., Tainan, Taiwan (2008).

[16] M. Sohgawa, T. Mima, H. Onishi, T. Kanashima, M. Okuyama, K. Yamashita, M. Noda, M. Higuchi, H. Noma, Tactile Array Sensor with Inclined Chromium/Silicon Piezoresistive Cantilevers Embedded in Elastomer, Transducers 2009, Denver CO, USA (2009) 284–287.

[17] M. Sohgawa, T. Uematsu, W. Mito, T. Kanashima, M. Okuyama, H. Noma, Crosstalk Reduction of Tactile Sensor Array with Projected Cylindrical Elastomer over Sensing Element, Jpn. J. Appl. Phys. 50 (2011) 06GM08.

[18] H. Onishi, M. Sohgawa, H. Tachibana, Y. M. Huang, T. Kanashima,

M. Okuyama, K. Yamashita, M. Noda, H. Noma, Stability Improvement of Tactile Sensor of Normal and Shear Stresses Using NiCr Thin Film Gauge, IEEJ Trans. on Sensors and Micromachines 129 (2009) 411–416.

[19] H. Tachibana, S. Kamanaru, T. Mima, M. Sohgawa, T. Kanashima, M. Okuyama, K. Yamashita, M. Noda, H. Noma, M. Higuchi, Fabrication and Basic Characteritics of Multiaxial Tactile Sensor with 3 Cantilevers, IEEJ Trans. on Sensors and Micromachines 130 (2010) 223–229.

[20] K. Hosokawa, I. Shimoyama, H. Miura, Two-dimensional micro-self-assembly using the surface tension of water, Sens. Act. 57 (1996) 117–125.

[21] Y. Arimitsu, First-time Material Mechanics (Hajimete no Zairyouriki-gaku), first ed., Kato Bunmeisha, Tokyo, 1999.

[22] T. Potma, Strain Gauges: Theory and Application, first ed., N. V. Philips' Gloeitampenfabrieken, Eindhoven, 1967.

[23] W. Mito, H. Yamazoe, S. Yoshida, M. Tada, M. Sohgawa, T. Kanashima, M. Okuyama, H. Noma, Gripping status classification using an array of micro cantilever type tactile sensor, Int. Conf.on Advanced Mechatronics, Osaka, Japan (2010) 351–354.

[24] W. Mito, T. Mima, H. Yamazoe, S. Yoshida, M. Tada, M. Sohgawa, T. Kanashima, M. Okuyama, H. Noma, Confirmation of Gripping Status Classfication using an Array of Micro Cantilever Type Tactile Sensor, Trans. SICE 47 (2011) 40–42.

Figure Captions

Fig. 1: The basic concept of the proposed tactile sensor, (a) a schematic view of structure of the tactile sensor, and (b) a cross-sectional structure of the microcantilever.

Fig. 2: An optical and a electron microscopic images of a tactile sensor element.

Fig. 3: Temperature coefficient of resistance of the NiCr thin film as a function of Cr weight concentration.

Fig. 4: The bimetallic structure model for calculation.

Fig. 5: Temperature coefficient of resistance of the NiCr thin film (Cr: 75wt%) before and after releasing the cantilever from the substrate, and that after embedded in the PDMS.

Fig. 6: Resistance changes of the tactile sensors with NiCr film of Cr: 20wt% and 75wt% as a function of (a) normal force and (b) shear force applied repeatedly.

Fig. 7: Comparison between applied forces in x, y, z axes and those measured by fabricated sensors with (a) the NiCr (Cr: 20wt%) and (b) NiCr (Cr: 75wt%) films.

Fig. 8: A schematic view and a photograph of the experimental system of slippage detection using fabricated tactile sensor array in the case of gripping of an acrylic object by the robotic hand.

Fig. 9: The Wheatstone birige circuit for detection of the gripping condition, (a) a schemitic circuit diagram, and (b) a photograph of the fabricated microcantilevers with reference resistances.

Fig. 10: Relationship between the output of the fabricated tactile sensor and gripping states of the robotic hand.

Table Captions

Table 1: Mechanical constants for calculation of the bimetallic effect.

Vitae

Masayuki Sohgawa was born in Wakayama, Japan, on April 4, 1977. He received the Ph. D. degree in engineering in 2005 from Osaka University. He is now a assistant professor at Graduate School of Engineering Science, Osaka University since 2007, working on MEMS physical sensors. He is a member of the Japan Society of Applied Physics and the Institute of Electrical Engineers of Japan.

Daiki Hirashima was born in 1987. He received the B. E. degree from Osaka University, Osaka, Japan, in 2010. He is M. student in the Graduate School of Engineering Science, Osaka University. He is engaged in research on tactile sensor devices.

Yusuke Moriguchi was born in 1988. He received the B. E. degree from Osaka University, Osaka, Japan, in 2011. He is now M. student in Nara Institute of Science and Technology.

Tatsuya Uematsu was born in 1988. He received the B. E. degree from Osaka University, Osaka, Japan, in 2010. He is M. student in the Graduate School of Engineering Science, Osaka University. He is engaged in research on tactile sensor devices.

Wataru Mito Wataru Mito was born in August 2, 1984. He received B.E. and M.E. degree from Kyoto Institute of Technology, Japan in 2009 and 2011. He is now joining SECOM Co., Ltd. as a researcher. He is a member of the SICE, IEICE and VRSJ.

Takeshi Kanashima was born in Japan on 1968. He received the M. E. and D. E. degrees from Department Electrical Engineering, Osaka University, Japan, in 1993 and 1996, respectively. He is associate professor now of Osaka University. His main field of research is thin film preparation of photo-assisted CVD, characterization of surface and interface, ferroelectric thin films and those applications such as memory. He is a member of the Japan Society of Applied Physics and the Japan Society for Synchrotron Radiation Research.

Masanori Okuyama received the B. S., M. S. and D. E. degrees in electrical engineering from Osaka University, Osaka Japan in 1968, 1970 and in 1973, respectively. He was a researcher of Japan Society for the Promotion of Science from 1973 to 1974 and a Research Associate the Faculty of Engineering Science, Osaka University, from 1974 to 1986, and Associate Professor from 1986 to 1991, and a Professor of Faculty of Engineering Science with Osaka University from 1991 to 2009. His current interests are preparation and characterization of ferroelectric thin films and their applications to electronic devices including memory devices, sensors and actuators, and characterization of gate insulator films on Si.

Haruo Noma received the B. E. degree and Ph.D. degree from University of Tsukuba, Ibaraki, Japan, in 1989 and 1994, respectively. In 1994, he joined ATR, where he was working on the force display, locomotion interface, their applications to the manipulation in virtual space, sensor network system, and MEMS sensor. He is members of the VRSJ, IEICE, RSJ, SICE, SICE, ACM and IEEE.

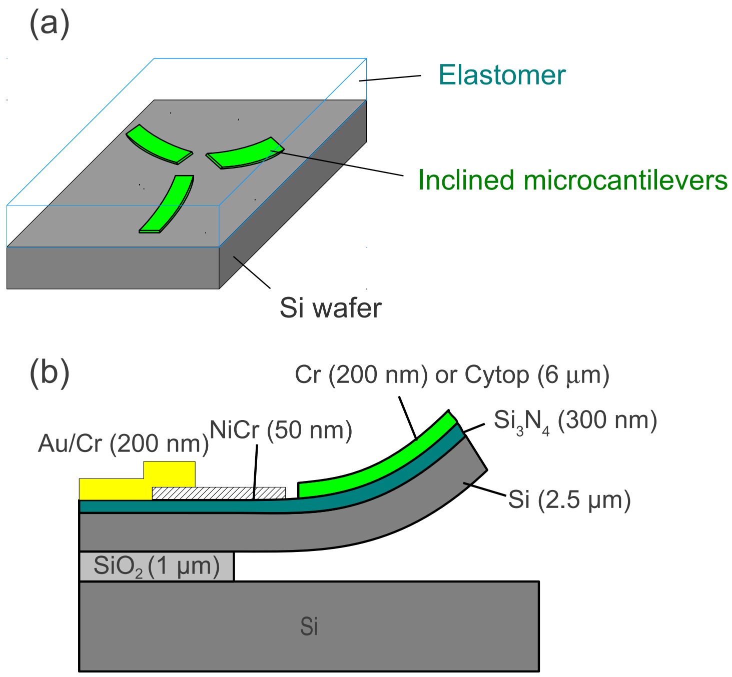
(a)
Elastomer
Inclined microcantilevers
Si wafer
(b)
Cr (200 nm) or Cytop (6 µm)
Si3N4 (300 nm)
Au/Cr (200 nm)
NiCr (50 nm)
Si (2.5 µm)
SiO2 (1 µm)
Si

Figure 1

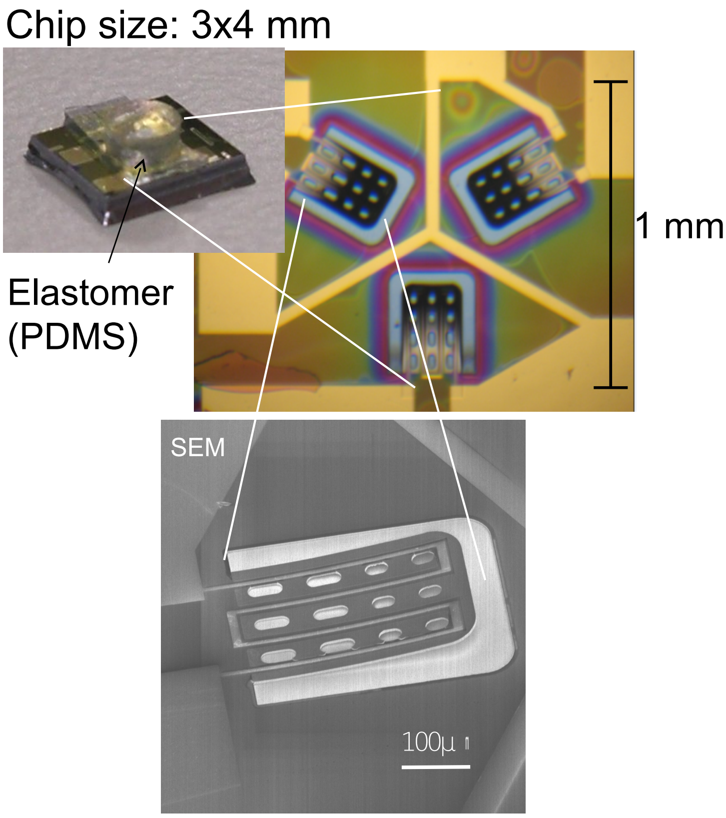

Figure 2

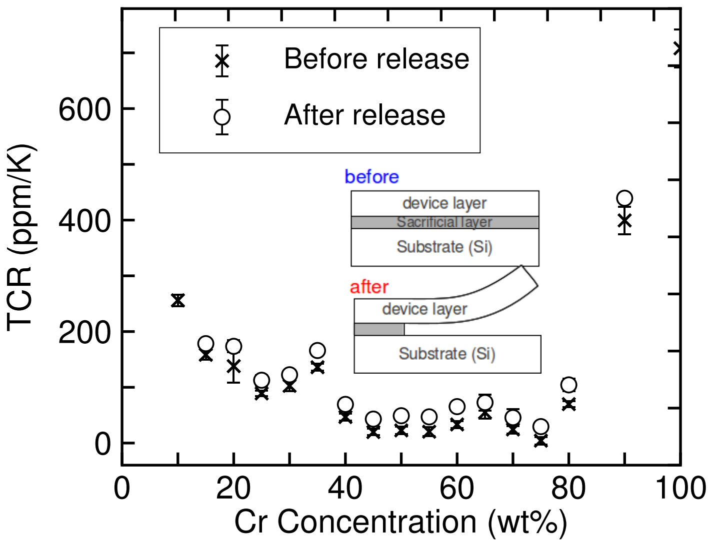

Before release
After release
before
device layer
Sacrificial layer
Substrate (Si)
after
device layer
Substrate (Si)
TCR (ppm/K)
Cr Concentration (wt%)
0
200
400
600
0
20
40
60
80
100

Figure 3

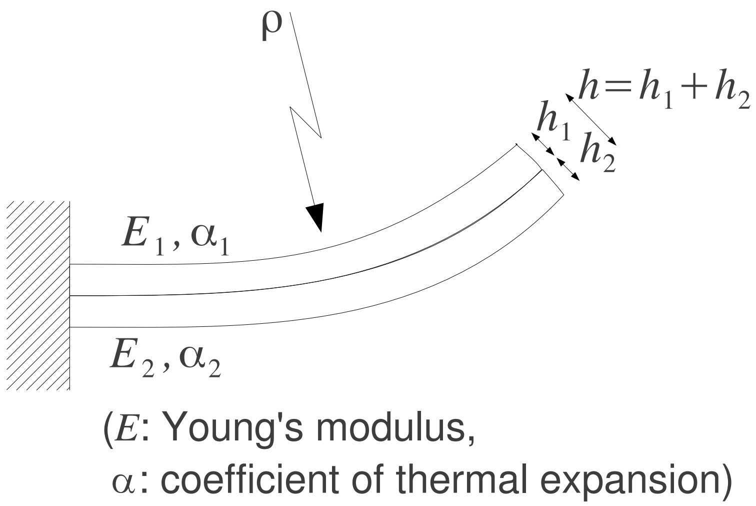

ρ
$h = h_1 + h_2$
h_1
h_2
E_1, α_1
E_2, α_2
(E: Young's modulus,
α: coefficient of thermal expansion)

Figure 4

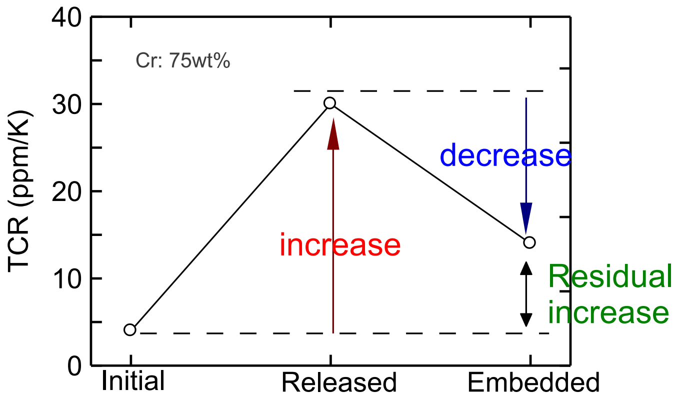
Cr: 75wt%
TCR (ppm/K)
40
30
20
10
0
Initial
Released
Embedded
increase
decrease
Residual
increase

Figure 5

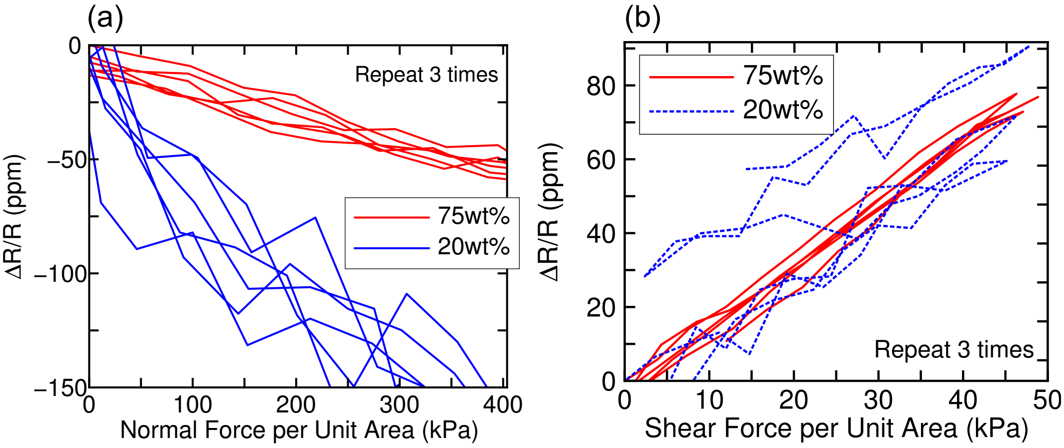
(a)
Repeat 3 times
75wt%
20wt%
ΔR/R (ppm)
0
−50
−100
−150
0
100
200
300
400
Normal Force per Unit Area (kPa)
(b)
75wt%
20wt%
Repeat 3 times
ΔR/R (ppm)
0
20
40
60
80
0
10
20
30
40
50
Shear Force per Unit Area (kPa)

Figure 6

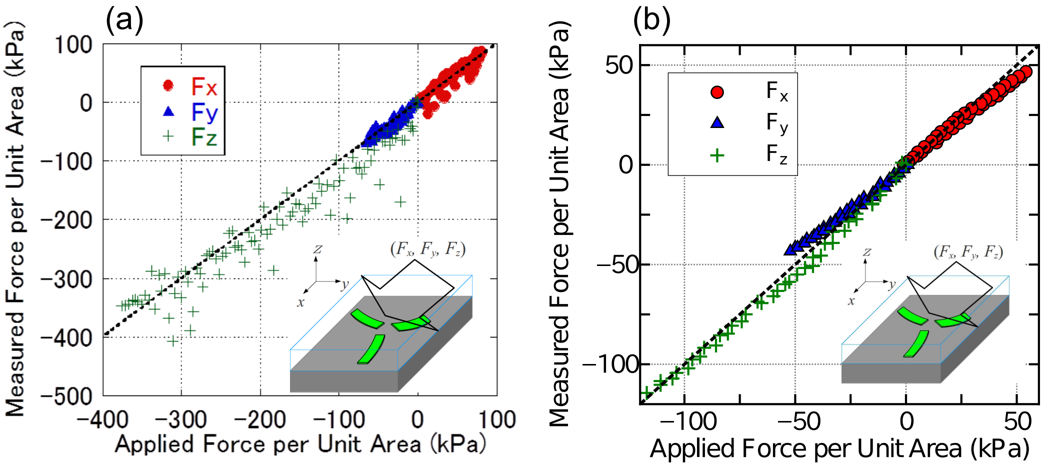

(a)
Fx
Fy
Fz
(F_x, F_y, F_z)
Measured Force per Unit Area (kPa)
Applied Force per Unit Area (kPa)
(b)
F_x
F_y
F_z
Measured Force per Unit Area (kPa)
Applied Force per Unit Area (kPa)

Figure 7

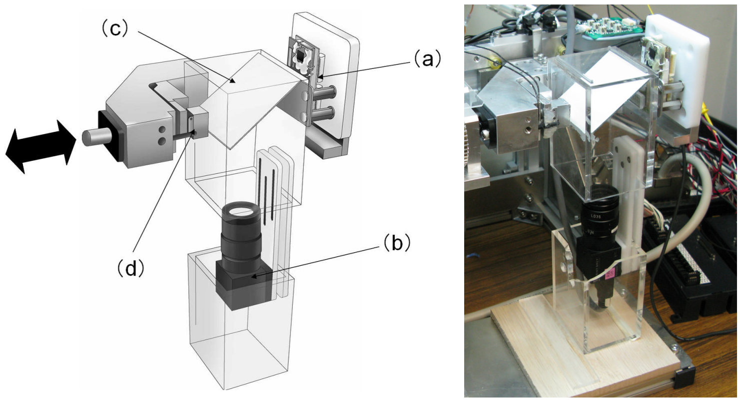

Figure 8

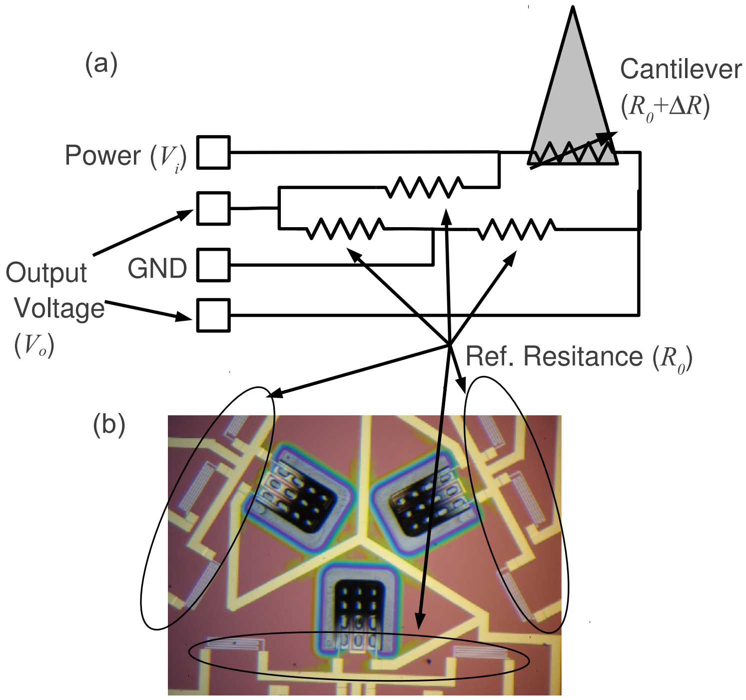
(a)
Cantilever
$(R_0+\Delta R)$
Power (V_i)
Output
Voltage
(V_o)
GND
Ref. Resitance (R_0)
(b)

Figure 9

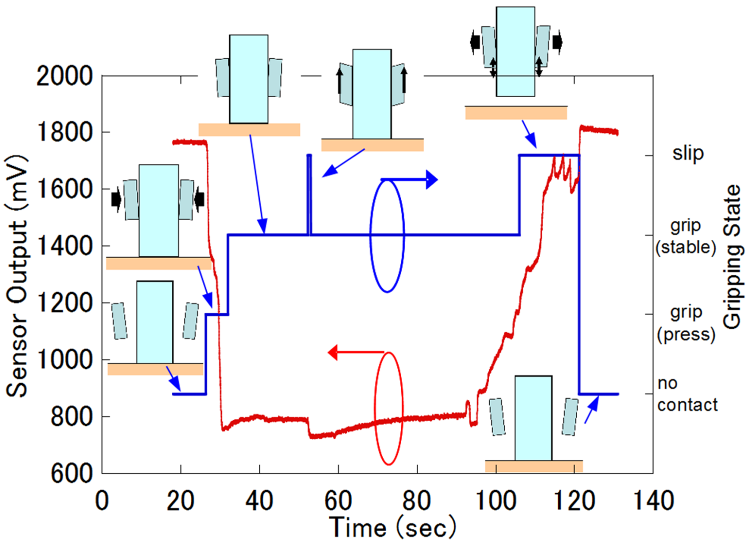
2000
1800
1600
1400
1200
1000
800
600
Sensor Output (mV)
0
20
40
60
80
100
120
140
Time (sec)
slip
grip
(stable)
grip
(press)
no
contact
Gripping State

Figure 10

Table 1

	CYTOP	Si
Young's modulus (GPa)	2.9	170
Coefficient of thermal expansion (ppm/K)	120	2.6